DESIGN, SYNTHESIS, CYTOTOXIC ACTIVITY AND DNA INTERCALATION OF NEW β-CARBOLINE DERIVATIVES

MAZLIN BINTI MOHIDEEN

UNIVERSITI SAINS MALAYSIA

2018

DESIGN, SYNTHESIS, CYTOTOXIC ACTIVITY AND DNA INTERCALATION OF NEW β-CARBOLINE DERIVATIVES

by

MAZLIN BINTI MOHIDEEN

Thesis submitted in fulfilment of the requirements
for the degree of
Doctor of Philosophy

June 2018

ACKNOWLEDGEMENT

First and foremost, I would like to thank Allah SWT, the Most Gracious and the Most Merciful without His blessings I would neither have begun nor completed my PhD degree program. Moreover, peace be upon our beloved Prophet Muhammad SAW.

A particular note of appreciation and sincere gratitude is extended to my supervisor, Prof. Dr Mohd Nizam bin Mordi (Centre for Drug Research, Universiti Sains Malaysia, USM) for his assistance and supervision, suggestions and constructive comments, given to me throughout this research project and encouragement during my work. A note of thanks is also forwarded to Prof. Dr Sharif bin. Mahsufi Mansor (Centre for Drug Research, Universiti Sains Malaysia USM) in his capacity as project leader, Assoc. Prof. Dr Melati binti Khairuddean, (School of Chemistry, Universiti Sains Malaysia, USM) as my co-supervisor, Dr Haslina binti Ahmad (Department of Science, Universiti Putra Malaysia, UPM) as my field supervisor and Assoc. Prof. Dr A. F. M. Motiur Rahman (Department of Pharmaceutical Chemistry, College of Pharmacy, King Saud University) for their advice and help throughout my research.

I would also like to take this opportunity to express my sincere gratitude to the Centre for Drug Research, Universiti Sains Malaysia (USM) for giving me the chance to pursue my PhD degree and in utilizing the Centre's facilities and at the same time expressing my gratitude to the Ministry of Higher Education (MOHE) for providing me with scholarship (My Brains 15 - My PhD as well as to USM's Research Creativity and Management Office (RCMO) for Research University Grant

Scheme for Team (RUT-1001/CDADAH/855055) for the completion of this research project.

My deepest appreciation and gratitude are also forwarded to Mr Zahari for helping in obtaining NMR analysis data from the School of Chemical Sciences, Universiti Sains Malaysia (USM), Universiti Teknologi MARA, campus Puncak Alam (UiTM) for thermal melting instruments and the Malaysian Genome Institute (MGI) for their circular dichroism (CD) instruments. Also, special thanks to all technicians and administrative staff of the Centre for Drug Research, especially Mr Hilman bin Sulaiman and Mr Rahim bin Ali Musa for their indispensable help in operating the mass spectrometry instruments

Finally, to my colleague, Miss Nur Azzalia binti Kamaruzaman, my parents and siblings for their support and those who have in one way or another contributed to the progress of this project and whom I have unintentionally omitted to mention here, thanks a lot for all that you have given. Most of all, I am very grateful to Allah SWT the only God I worship, for blessing me with good health in completing this study.

Mazlin Binti Mohideen
June 2018

TABLES OF CONTENTS

ACKNOWLEDGEMENT **ii**

TABLE OF CONTENTS **iv**

LIST OF TABLES **ix**

LIST OF FIGURES **xi**

LIST OF SCHEMES **xvi**

LIST OF SYMBOLS **xvii**

LIST OF ABBREVIATIONS **xx**

ABSTRAK **xxv**

ABSTRACT **xxvii**

CHAPTER 1: INTRODUCTION **1**

1.1 Cancer 1

1.2 DNA intercalating agents 3

1.2.1 The anthracycline antitumor agents 4

1.3 Problem statement 6

1.4 Scope of study 7

1.5 Objectives 8

CHAPTER 2: LITERATURE REVIEW **9**

2.1 Background of β-carboline 9

2.2 Synthesis of β-carboline derivatives 13

2.2.1 Precursors in the synthesis of β-carbolines 13

2.2.2 Conventional synthetic methods of β-carbolines 14

2.2.3 The aromatization of β-carboline system 16

2.3 Pharmacological effects of β-carbolines *in vitro* 22

2.4 Evaluation of *in vitro* cytotoxicity 29

2.4.1 MTT [3-(4,5-dimethylthiazol-2-yl)-2,5-diphenyltetrazolium bromide] colourimetric assay 30

2.4.2 Erythroleukemia: K562 cell line as model for *in vitro* cytotoxicity study 31

2.5 3D-QSAR and molecular docking of β-carboline derivatives 32

2.6 Biochemical effects and pharmacodynamic of β-carboline derivatives and DNA interactions at molecular level 34
2.6.1 Overview of DNA 35
2.6.2 DNA-structure and specificity 36
2.6.3 DNA-drug interactions 37
2.6.3(a) Intercalation binding mode 38
2.6.4 DNA-drug intercalation and applications 39
2.6.4(a) Thermal stability and denaturation of DNA 43
2.6.4(b) UV-Visible absorption spectroscopy 46
2.6.4(c) Fluorescence emission spectroscopy 49
2.6.4(d) Circular dichroism (CD) spectroscopy 51

CHAPTER 3: METHODOLOGY 53
3.1 Development of 3D-QSAR models 53
3.1.1 Software 53
3.1.2 Dataset 53
3.1.3 Molecular optimisation and conformational analysis 54
3.1.4 Generation alignment-independent molecular descriptors (GRIND-2) analysis 56
3.2 Synthesis and characterisation of compounds 58
3.2.1 Chemicals/solvents or reaction application general remarks 58
3.2.2 Chromatography 61
3.2.2(a) Thin-Layer Chromatography (TLC) 61
3.2.2(b) Column chromatography 62
3.2.3 Compound identification and structure elucidation 62
3.2.3(a) Gas Chromatography-Mass Spectrometry (GC-MS) 62
3.2.3(b) Electrospray Ionization-Mass Spectroscopy (ESI-MS) 62
3.2.3(c) Fourier Transform Infrared Spectroscopy (FT-IR) 63
3.2.3(d) Nuclear Magnetic Resonance (NMR) 63
3.2.3(e) Elemental analysis 64
3.2.3(f) Melting point 64
3.2.4 Synthesis of β-carboline derivatives 64
3.2.4(a) General procedure for the preparation of 1-substituted- 66

1,2,3,4-tetrahydro-β-carboline-3-carboxylic acid (**M1-M3**)

3.2.4(b) General procedure for the preparation of ethyl 1-substituted-1,2,3,4-tetrahydro-β-carboline-3-carboxylate (**M4-M6**) 68

3.2.4(c) General procedure for the preparation of ethyl 1-substituted-β-carboline-3-carboxylates (**M7-M9**) 70

3.2.4(d) General procedure for the preparation of ethyl 9-substituted-β-carboline-3-carboxylate (**M10-M16**) and 2,9-disubstituted-β-carbolineum bromide (**M47-M53**) 73

3.2.4(e) General procedure for the preparation 1,9-disubstituted-β-carboline-3-carboxylate (**M17-M20**) 77

3.2.4(f) General procedure for the preparation of 1-substituted-β-carboline (**M21-M22**) 80

3.2.4(g) General procedure for the preparation of 2-substituted-β-carbolineum bromide (**M23-M46**) 81

3.2.4(h) General procedure for the preparation of 1,2,9-trisubstituted β-carbolineum bromide (**M47-M113**) 94

3.2.5 Experimental details for single-crystal structure determination 134

3.3 Cytotoxic evaluation of the synthesised compounds 134

3.3.1 Materials/reagents and equipment 134

3.3.2 Preparation of culture media and phosphate buffer saline (PBS) 136

3.3.3 Cell line processing and maintenance 137

3.3.4 Resuscitation of cryopreserved cells 137

3.3.5 Culture conditions 138

3.3.6 Cell quantification 139

3.3.7 Preparation of compound's stock solutions 140

3.3.8 Preparation of working MTT solution stock 140

3.3.9 MTT assay protocol 141

3.3.10 Primary and secondary screenings 142

3.4 Drug-DNA intercalations 143

3.4.1 Chemicals and reagents 143

3.4.2 Preparations of stock solution of CT-DNA 144

3.4.3 Instruments and experimental techniques 144
3.4.3(a) DNA thermal denaturation studies 144
3.4.3(b) UV-Visible absorption spectroscopy 145
3.4.3(c) Fluorescence emission spectroscopy 146
3.4.3(d) Circular dichroism (CD) spectroscopy 147
3.5 Molecular docking 148
3.5.1 Materials and methods 148
3.5.2 Visualization and Docking tools 149
3.5.2(a) Protein Data Bank (PDB) 149
3.5.2(b) Preparation of ligand molecules 149
3.5.2(c) Preparation of receptor macromolecule 149
3.5.2(d) Calculation of grid maps 151
3.5.2(e) Docking simulation (using AutoDock 4.0) 151

CHAPTER 4: RESULTS AND DISCUSSION 152
4.1 Development of 3D-QSAR model using previous literature data 152
4.1.1 Principal component analysis (PCA) analysis of the dataset 153
4.1.2 Partial least square (PLS) analysis of 3D-QSAR model 154
4.1.3 Data interpretation for 3D-QSAR model using PLS coefficients plot 160
4.2 Synthesis of β-carbolineum derivatives 166
4.2.1 Synthesis of N^2,N^9-benzylated-β-carboline derivatives 167
4.2.1(a) Structural characterisation of compound **M14** 171
4.2.1(b) Structural characterisation of compound **M51** 175
4.2.2 Synthesis of N^9-β-carboline-3-carboxylate ester 181
4.2.2(a) Structural characterisation of compound **M19** 183
4.2.2(b) Structural characterisation of compound **M20** 185
4.2.3 Synthesis of N^2,N^9-benzylated-1-substituted quaternary β-carbolineum bromate derivatives 187
4.2.3(a) Discussion on the synthesis of 1-substituted-β-carboline 188
4.2.3(b) Discussion on the new synthesis of N^2,N^9-benzylated-1-substituted-β-carbolineum bromate derivatives 189

4.2.3(b)(i) Structural characterisation of compound **M44** 195
4.2.3(b)(ii) Structural characterisation of compound **M108** 199
4.3 Biological evaluation of the synthesised compounds 205
4.4 Structure-activity relationship (SAR) consideration 214
4.5 Interactions of β-carboline derivatives with CT-DNA 218
4.5.1 DNA Thermal denaturation studies 219
4.5.2 UV-Visible absorption spectroscopy 221
4.5.3 Fluorescence emission spectroscopy using indirect evolution of interaction 229
4.5.4 Circular dichroism (CD) spectroscopy analysis 235
4.5.5 Visual representation of drug-DNA complex using molecular docking 241

CHAPTER 5: CONCLUSION **247**
5.1 Future studies 248

REFERENCES **250**

APPENDICES

LIST OF TABLES

		Page
Table 3.1	List of programs and their software packages	53
Table 3.2	Structures and cytotoxic activity (experimental pIC_{50}) toward HepG2 cancer cell line for 3D-QSAR model	55
Table 3.3	List of solvents, chemicals and material used in synthesis and structural characterization	59
Table 3.4	List of equipment used in cytotoxicity study	135
Table 3.5	List of materials and reagents used in cytotoxicity study	136
Table 3.6	List of materials and reagents used in drug-DNA intercalations study	143
Table 3.7	List of programs and their software packages used in molecular docking	148
Table 4.1	PCA statistic for the dataset toward HepG2 cell line	153
Table 4.2	PLS statistic for the dataset using Leave-One-Out (LOO) toward HepG2 cell line after 2 FFD cycle	155
Table 4.3	Predicted activity with their residual values for dataset (n = 25) using 3D-QSAR model built toward HepG2 cell line	156
Table 4.4	Statistics of PLS model in training set toward HepG2 cell line after 2 FFD cycle	157
Table 4.5	Predicted activity with their residual values for training set (n = 20) using 3D-QSAR model built toward HepG2 cell line	159
Table 4.6	Summary of GRID-independent descriptors that are highly correlated to cytotoxic activity of β-carboline derivatives using HepG2 cell line	165
Table 4.7	Optimisation of reaction conditions for compounds **M51** and **M14**	169
Table 4.8	Synthesis of compounds **M10-M16** and **M47-M53**	170
Table 4.9	1D- and 2D-NMR data of compound **M14**	175
Table 4.10	1D- and 2D-NMR data of compound **M51**	180
Table 4.11	Optimization of reaction conditions compounds **M17-M20**	182
Table 4.12	Optimization of reaction conditions for compound **M21**	189

Table 4.13	Optimization of reaction conditions for compounds **M44**, **M51** and **M108**	190
Table 4.14	Synthesis of N^2-benzylated-β-carbolineum bromate derivatives (**M23**-**M46**)	192
Table 4.15	Synthesis of N^2,N^9-benzylated-1-substituted-β-carbolineum bromate derivatives (**M47**-**M113**)	193
Table 4.16	1D- and 2D-NMR data of compound **M44**	199
Table 4.17	1D- and 2D-NMR data of compound **M108**	204
Table 4.18	Chemical structures and the IC_{50} of β-carboline derivatives against cancer and non-cancerous cell lines (μM)	208
Table 4.19	Thermal denaturation data of T_m and ΔT_m for compounds - binding with calf thymus DNA (CT-DNA). Ratio of [DRUG] / [DNA] = 1:5	220
Table 4.20	Binding constants for the complexes of DOX, HAR, 5-FU, **M53** and **M56** with CT-DNA calculated from UV-Vis spectroscopy data at T = 309.5 K, pH = 7.4	228
Table 4.21	Fluorescence emission spectra of EtBr-DNA in the presence of increasing amounts of DOX, HAR, 5-FU, **M53** and **M56** with DNA at T = 309.5 K, pH = 7.4	235

LIST OF FIGURES

		Page
Figure 1.1	Intercalation of ethidium bromide into-double-stranded DNA, showing lengthening of the DNA helix (reproduced from Watson, 1987)	3
Figure 1.2	The antitumor anthracycline doxorubicin	4
Figure 1.3	The chemical structure of harmine	6
Figure 2.1	Numbering of the β-carboline (**1**) skeleton	9
Figure 2.2	*Peganum harmala* (adapted from Asgarpanah & Ramenzanloo, 2012)	10
Figure 2.3	Structures of β-carbolines (**1**, **2**, **3** and **4**), dihydro-β-carbolines (DHβCs) (**5**, **6** and **7**) and tetrahydro-β-carboline (THβC) (**8**) alkaloids	12
Figure 2.4	Precursors used in the synthesis of β-carbolines	13
Figure 2.5	The structure-activity relationships (SARs) of β-carboline derivatives against tumour cells (Cao et al., 2007)	28
Figure 2.6	Reduction of 3-(4,5-dimethyl-2-thiazolyl)-2-5-diphenyl-2*H*-tetrazolium bromide (MTT) to a formazan	31
Figure 2.7	The structure of the DNA double helix (adapted from Leslie & Pray, 2008)	35
Figure 2.8	Watson-Crick base pair (adenine, cytosine, guanine and thymine) (adapted from Raiber et al., 2017)	36
Figure 2.9	The melting curve of DNA (adapted from National Programme on Technology Enhanced Learning (NPTEL), 2014)	45
Figure 2.10	Diagrammatic representation of the thermal melting process (adopted from Fatima et al., 2013)	46
Figure 2.11	Shifts and effect on a chromophore in UV-Visible spectroscopy (adapted from National Programme on Technology Enhanced Learning (NPTEL), 2014)	48
Figure 3.1	Counting regions of viable cells vy (**a**, **b**, **c**, **d**) improved Neubauer haemocytometer	140
Figure 3.2	Grid box structure of the receptor (1D12) and the ligand (DOX)	151

Figure 4.1	PCA scores plot of PC1 *vs* PC2, for dataset toward HepG2 cell line	154
Figure 4.2	Plot of actual activity *vs.* predicted activity pIC_{50} values of dataset toward HepG2 cell line	156
Figure 4.3	Plot of actual activity *vs* predicted activity pIC_{50} values of external test set toward HepG2 cell line	160
Figure 4.4	PLS Coefficients correlogram is showing the descriptors which are directly (positive values) or inversely (negative values) correlated to the cytotoxic activity. The activity predominantly increases with the increase in DRY-DRY, TIP-TIP and DRY-TIP descriptor values	161
Figure 4.5	Schematic (a-f) representation the most important variable of the 3D-QSAR model using HepG2 cell line: (a) DRY-DRY 25 (10.0-10.4 Å); (b) TIP-TIP 166 (2.8-3.2 Å); (c) TIP-TIP 201 (16.8-17.2 Å); (d) DRY-TIP 356 (15.2-15.5 Å); (e) DRY-TIP 348 (12.0-12.4 Å); (f) DRY-TIP 336 (7.2-7.6 Å). Yellow and green circles represent hydrophobic (DRY) and shape (TIP) regions, respectively. Red and blue lines represent the variables with positive and negative impact, respectively. Å represents the spatial distance between the connected nodes	164
Figure 4.6	The summary of structural requirements of β-carboline as predicted from model using HepG2 cell line	166
Figure 4.7a	^{1}H-NMR spectrum of compound **M14** (500 MHz, $CDCl_3$)	172
Figure 4.7b	^{13}C-NMR spectrum of compound **M14** (125 MHz, $CDCl_3$)	172
Figure 4.7c	COSY spectrum of compound **M14**	174
Figure 4.8	ESI-MS spectrum of compound **M51**	176
Figure 4.9a	^{1}H-NMR spectrum of compound **M51** (500 MHz, $CDCl_3$)	177
Figure 4.9b	^{13}C-NMR spectrum of compound **M51** (125 MHz, $CDCl_3$)	177
Figure 4.9c	COSY spectrum of compound **M51**	179
Figure 4.10	ESI-MS spectrum of compound **M19**	184
Figure 4.11a	^{1}H-NMR spectrum of compound **M19** (500 MHz, $CDCl_3$)	184
Figure 4.11b	^{13}C-NMR spectrum of compound **M19** (125 MHz, $CDCl_3$)	185
Figure 4.12a	^{1}H-NMR spectrum of compound **M20** (500 MHz, $CDCl_3$)	186
Figure 4.12b	^{13}C-NMR spectrum of compound **M20** (125 MHz, $CDCl_3$)	186

Figure 4.13	ESI-MS spectrum of compound **M44**	195
Figure 4.14a	^{1}H-NMR spectrum of compound **M44** (500 MHz, $CDCl_3$)	196
Figure 4.14b	^{13}C-NMR spectrum of compound **M44** (125 MHz, $CDCl_3$)	196
Figure 4.14c	COSY spectrum of compound **M44**	198
Figure 4.15	ESI-MS spectrum of compound **M108**	200
Figure 4.16a	^{1}H-NMR spectrum of compound **M108** (500 MHz, $CDCl_3$)	201
Figure 4.16b	^{13}C-NMR spectrum of compound **M108** (125 MHz, $CDCl_3$)	201
Figure 4.16c	COSY spectrum of compound **M108**	203
Figure 4.17	A melting curve that showed thermal denaturation curves of free CT-DNA (50 µM) which was dissolved in PBS pH 7.4. Data was presented as $(A\text{-}A_0)/(A_f\text{-}A_0)$ *versus* temperature, where A_f, A_0, and A are the final, initial and observed absorbances at 260 nm respectively	219
Figure 4.18	The UV-Vis spectrum of CT-DNA in 0.01 M PBS solution [Purity of CT-DNA (A_{260}/A_{280}) = 1.83; Concentration of CT-DNA (A_{260}/6600) = 1.06 x 10^{-4} M]	221
Figure 4.19	Absorption spectra of DOX in the presence of increasing amounts of CT-DNA (C_{DOX} = 10 µM; C_{DNA} = 2-34 µM). The arrow indicates that absorbance changes upon increasing DNA concentrations; Insert: Linear plot for the calculation of intrinsic binding constant (K_b)	223
Figure 4.20	Absorption spectra of 5-FU in the presence of increasing amounts of CT-DNA ($C_{5\text{-}FU}$ = 10 µM; C_{DNA} = 2-32 µM). The arrow indicates that absorbance changes upon increasing DNA concentrations; Insert: Linear plot for the calculation of intrinsic binding constant (K_b)	224
Figure 4.21	Absorption spectra of HAR in the presence of increasing amounts of CT-DNA (C_{HAR} = 10 µM; C_{DNA} = 2-40 µM). The arrow indicates that absorbance changes upon increasing DNA concentrations; Inset: Linear plot for the calculation of intrinsic binding constant (K_b)	225
Figure 4.22	Absorption spectra of **M53** in the presence of increasing amounts of CT-DNA ($C_{\mathbf{M53}}$ = 10 µM; C_{DNA} = 2-36 µM). The arrow indicates that absorbance changes upon increasing DNA concentrations; Inset: Linear plot for the calculation of intrinsic binding constant (K_b)	227

Figure 4.23	Absorption spectra of **M56** in the presence of increasing amounts of CT-DNA ($C_{\mathbf{M56}}$ = 10 μM; C_{DNA} = 2-38 μM). The arrow indicates that absorbance changes upon increasing DNA concentrations; Inset: Linear plot for the calculation of intrinsic binding constant (K_b)	227
Figure 4.24	Fluorescence emission spectra of EtBr in the presence of increasing amounts of CT-DNA (C_{EtBr} = 20 μM; C_{DNA} = 2-20 μM). The arrow indicates that absorbance changes upon increasing DNA concentrations	230
Figure 4.25	Fluorescence emission spectra of EtBr-DNA in the presence of increasing amounts of DOX (C_{DOX} = 0.1-1.4 μM). The arrow indicates that absorbance changes upon increasing DOX concentrations; Insert: Stern-Volmer plot for the calculation of quenching constant (K_{sv})	231
Figure 4.26	Fluorescence emission spectra of EtBr-DNA in the presence of increasing amounts of 5-FU ($C_{5\text{-}FU}$ = 2-44 μM). The arrow indicates that absorbance changes upon increasing 5-FU concentrations; Inset: Stern-Volmer plot for the calculation of quenching constant (K_{sv})	231
Figure 4.27	Fluorescence emission spectra of EtBr-DNA in the presence of increasing amounts of HAR (C_{HAR} = 2-42 μM). The arrow indicates that absorbance changes upon increasing HAR concentrations; Inset: Stern-Volmer plot for the calculation of quenching constant (K_{sv})	233
Figure 4.28	Fluorescence emission spectra of EtBr-DNA in the presence of increasing amounts of compound **M53** ($C_{\mathbf{M53}}$ = 2-90 μM). The arrow indicates that absorbance changes upon increasing compound **M53** concentrations; Inset: Stern-Volmer plot for the calculation of quenching constant (K_{sv})	234
Figure 4.29	Fluorescence emission spectra of EtBr-DNA in the presence of increasing amounts of compound **M56** ($C_{\mathbf{M56}}$ = 2-48 μM). The arrow indicates that absorbance changes upon increasing compound **M56** concentrations; Inset: Stern-Volmer plot for the calculation of quenching constant (K_{sv})	234
Figure 4.30	Circular dichroism spectra of the free CT-DNA (C_{DNA} = 50 μM) in 0.01 M PBS	236
Figure 4.31	Circular dichroism spectra of the free CT-DNA (C_{DNA} = 50 μM) and DOX-DNA (C_{DOX} = 0.1-1.0 μM) in 0.01 M PBS	236
Figure 4.32	Circular dichroism spectra of the free CT-DNA (C_{DNA} = 50	237

µM) and and 5-FU-DNA ($C_{5\text{-}FU}$ = 0.1-0.4 µM) in 0.01 M PBS

Figure 4.33 Circular dichroism spectra of the free CT-DNA (C_{DNA} = 50 µM) and HAR-DNA (C_{HAR} = 1.0-6.0 µM) in 0.01 M PBS 239

Figure 4.34 Circular dichroism spectra of the free CT-DNA (C_{DNA} = 50 µM) and compound **M53**-DNA ($C_{\mathbf{M53}}$ = 0.1-0.8 µM) in 0.01 M PBS 240

Figure 4.35 Circular dichroism spectra of the free CT-DNA (C_{DNA} = 50 µM) and compound **M56**-DNA ($C_{\mathbf{M56}}$ = 5-25 µM) in 0.01 M PBS 240

Figure 4.36 Superimposition in DNA-intercalation site of original ligand DOX (DM 27) confirmation from docking and actual original ligand conformation with RMSD 1.72 Å 242

Figure 4.37 Prediction of docked complex of compound **M53** with DNA [PDB ID: 1D12] 244

Figure 4.38 Prediction of docked complex of compound **M56** with DNA [PDB ID: 1D12] 245

Figure 4.39 3D model of the intercalation mode of compounds **M53** and **M56** on double strand DNA represented by the molecular surface 246

LIST OF SCHEMES

		Page
Scheme 2.1	Summary of conventional synthetic methods of β-carbolines (**1**)	14
Scheme 2.2	Mechanism reaction of compound **8** using Pictet-Spengler reaction	15
Scheme 2.3	A Bischler-Napieralski cyclisation and reduction of DHβC (**12**)	16
Scheme 2.4	A plausible mechanism for the one-pot conversions of *N*-tosyl-THBCs (**13**) into β-carbolines (**14**) through tandem β-elimination and aromatization reactions	18
Scheme 2.5	IBX-mediated aromatization in the total synthesis of Eudistomin U (**17**)	19
Scheme 2.6	Proposed mechanism for copper-mediated decarboxylation and aromatization of THβCAs (**18**)	20
Scheme 2.7	A possible reaction mechanism for the decarboxylation aromatization of THβCs (**19**)	21
Scheme 2.8	Synthesis of β-carbolines (**20**) from THβCs (**21**) using iodobenzene diacetate	21
Scheme 3.1	Overall synthetic pathways for various series of β-carboline derivatives (**M1-M113**) prepared in this research	65
Scheme 4.1	Synthesis of 2,9-dibenzyl-3-ethoxycarbonyl-β-carbolineum bromate (**R1**)	167
Scheme 4.2	Synthesis of compounds **M51** and **M14**	168
Scheme 4.3	Synthesis of compounds **M17-M20**	181
Scheme 4.4	Synthesis of 1-substituted-β-carboline derivatives (**M21-M22**)	188

LIST OF SYMBOLS

A	Absorbance
Å	Angstrom
β	Beta
ε	Molar absorptivity
δ	Delta/Chemical shift in NMR
π	Pi
λ	Lambda
ΔT_m	Melting temperature
°C	Degree Celsius
%	Percentage
^1H	Proton
^{13}C	Carbon-13
1D	One-dimensional
2D	Two-dimensional
3D	Three-dimensional
acc	Accumulative value
br	Broad signal
cm^{-1}	Reciprocal centimetre (unit of wavenumber)
cm^2	Square centimetre
cm^3	Cubic centimetre
d	Doublet
dd	Doublet of doublet
dt	Doublet of triplet
ED_{50}	Median effective dose
E_{el}	Electrostatic energy
E_{hb}	Hydrogen bond energy
E_{lj}	Lennard-Jones energy
et al.	Elsewhere or/and other
eV	Electron volt
E_{xyx}	Interaction energy
F	Fluorescence intensity

g	Gram
h	Hour
Hz	Hertz
I	Fluorescence intensity
IC_{50}	50% Inhibition concentration
J	Coupling constant
K_b	Binding affinity
K	Kelvin
kcal	Kilocalories
K_{sv}	Stern-Volmer quenching constant
L	Litre
Lit.	Literature
log *P*	Logarithm of partition coefficient
m	Multiplet
M	Molar concentration
mg	Milligram
MHz	Megahertz
min	Minute
mL	Millilitre
mm	Millimetre
mM	Millimolar
mm^2	Square millimetre
mm^3	Cubic millimetre
mol	Mole
mmol	Millimole
m.p.	Melting point
m/z	Mass-to-charge ratio
n	Number of replicates
nm	Nanomolar
OD	Optical density
p	Probability value
pH	Potential of hydrogen
pIC_{50}	Negative logarithm values of IC_{50}

ppm	Parts per million
Q	Concentration of the quencher values
q	Quartet
r^2	Correlation coefficient
q^2	Cross-validation correlation coefficient
rpm	Rotations per minute
rt	Room temperature
s	Singlet
T	Temperature
t	Triplet
td	Triplet of doublet
µg	Microgram
µl	Microlitre
µmol	Micromole
µM	Micromolar
<	Less than
>	More than
=	Equal
±	Plus/Minus

LIST OF ABBREVIATIONS

βCs	β-carbolines
1A9	Human ovarian carcinoma cell line
769-P, 786-0, OS-RC-2	Human renal carcinoma cell line
5-FU	5-Fluorouracil
5-HT_{2A}	5-Hydroxytryptamine receptor 2A
5-HT_{2C}	5-Hydroxytryptamine receptor 2C
22RV1	Human prostate carcinoma epithelial cell line
A	Adenine
A375	Human malignant melanoma cell line
A549	Human lung adenocarcinoma epithelial cell line
AT	Adenine-thymine
ATCC	American Type Culture Collection
ATR	Attenuated total reflectance
BALB/3T3 clone A31	Mouse embryonic fibroblast
BCR:ABL	*Philadelphia* chromosome
Bel-7402	Human hepatocellular carcinoma cell line
BGC-823	Human gastric cancer cell line
C	Cytosine
CD	Circular dichroism
$CDCl_3$	Deuterated chloroform
CDK	Cyclin-dependent kinase
CD_3OD	Deuterated Methanol
CG	Cytosine-guanine
$CHCl_3$	Chloroform
CH_2Cl_2/DCM	Dichloromethane
CHN	Carbon, hydrogen and nitrogen
CIS	Cisplatin
CLACC	Consistently large auto and cross-correlation
CML (K562)	Human chronic myelogenous leukaemia cell line
CNS	Central nervous system
CO_2	Carbon dioxide

COSY	Correlation spectroscopy
CT-DNA	Calf thymus DNA
$Cu(OAc)_2$	Copper(II) acetate
$CuCl_2$	Copper(II) chloride
DCM	Dichloromethane
DDQ	2,3-dichloro-5,6-dicyano-1,4-benzoquinone
DEPT	Distortionless enhancement by polarisation transfer
DHβCs	Dihydro-β-carbolines
DMEM	Dulbecco's modified eagle's medium
DMF	Dimethylformamide
DMSO	Dimethyl sulfoxide
DMSO-d_6	Deuterated dimethyl sulfoxide
DOX	Doxorubicin
DNA	Deoxyribonucleic acid
ds-DNA	Double-strand DNA
Eca-109	Cellosaurus cell line
EDG	Electron-donating group
EDTA	Ethylenediaminetetraacetic acid
EI	Electron impact
ESI	Electrospray ionisation
EtBr	Ethidium bromide
Et_2O	Diethyl ether
EtOAc	Ethyl acetate
EtOH	Ethanol
EWG	Electron-withdrawing group
FBS	Fetal bovine serum
FDOX	*N*-(trifluoroacetyl) doxorubicin
FFD	Fractional factorial design
FT-IR	Fourier transform infrared spectroscopy
G	Guanine
GC	Gas chromatography
GC-MS	Gas chromatography-mass spectroscopy
GRIND	GRid-INdependent descriptors

GRIND-2	Second generation GRid-INdependent descriptors
HAR	Harmine
HBA	Hydrogen bond acceptors
HBD	Hydrogen bond donors
Hela	Human cervical carcinoma cell line
HepG2	Liver hepatocellular carcinoma cell line
HL-60	Human promyelocytic leukaemia cell line
HMBC	Heteronuclear multiple-bond coherence
HMQC	Heteronuclear multiple quantum coherence
H_2O	Water
H_2SO_4	Sulphuric acid
HSQC	Heteronuclear single quantum coherence
HT-29	Human colorectal adenocarcinoma cell line
IARC	International Agency for Research on Cancer
IBX	2-Iodoxybenzoic acid
IMDM	Iscove's modified Dulbecco's medium
ISO	International Organisation of Standardization
IUPAC	The International Union of Pure and Applied Chemistry
K562	Human immortalised myelogenous leukemia cell line
KB	Human LoVo colon carcinoma cell line
K_2CO_3	Potassium carbonate
LGA	Lamarckian Genetic Algorithm
LLC	Lewis lung carcinoma
LOO	Leave-one-out
Lovo	Human nasopharynx carcinoma cell line
LV	Latern variable
MACC	Maximum auto and cross-correlation
MCF-7	Human breast adenocarcinoma cell line
MeOH	Methanol
MIF	Molecular interaction fields
MM^+	Molecular mechanics
MMFF94	Merck Molecular Force Field
MnO_2	Manganese dioxide

MS	Mass spectrometry
MTT	3-(4,5-Dimethylthiazol-2-yl)-2,5-diphenyl tetrazolium bromide
NaCl	Sodium chloride
NaH	Sodium hydride
$NaHCO_3$	Sodium bicarbonate
NaOH	Sodium hydroxide
Na_2SO_4	Sodium sulphate
NCI	U.S National Cancer Institute
NCS	*N*-chloro-succinimide
NMR	Nuclear magnetic resonance spectroscopy
OVCAR-03	Human ovarian carcinoma cell line
P-388 and L-1210	Phosphoprotein p53
PBS	Phosphate-buffered saline
PCA	Principal component analysis
PC-3	Human prostate cancer cell line
PCl_5	Phosphorus pentachloride
PCs	Principal components
PDB	Protein Data Bank
Pearson-R	*Pearson* correlation coefficient
PLA-801	Human cell lung cancer cell line
PLK	Polo-like kinase
PLS	Partial-least square
$POCl_3$	Phosphoryl chloride
QSAR	Quantitative structure-activity relationship
R&D	Research and development
RM1	Recife Model 1
RMS	Root-mean-square
RMSE	Root-mean-square error
SaOS-2	Human osteosarcoma cell line
SARs	Structure-activity relationships
SCaBER	Bladder squamous carcinoma
SD	Standard deviation

SDEC	Standard deviation of the error of calculation
SDEP	Standard deviation of the error of predictions
SI	Selectivity Index
SKC01	Colon carcinoma
SK-MEL-2	Malignant melanoma cell line
SK-OV-3	Human ovarian cancer cell line
$SOCl_2$	Thionyl chloride
ss-DNA	Single-strand DNA
SSX	Percentage of the X sum of squares
(SW) kNN MFA	Step-Wise K-nearest neighbour molecular field analysis
T	Thymine
THβCs	Tetrahydro-β-carbolines
THβCAs	Tetrahydro-β-carboline-3-carboxylic acid
THF	Tetrahydrofuran
TLC	Thin-layer chromatography
TMS	Tetramethylsilane
U-87-MG	Human primary glioblastoma cell line
U251	Human malignant glioma cell line
UACC-62	Cellosaurus cell line
UK	United Kingdom
USA	The United States of America
UV-Vis	Ultraviolet-visible spectroscopy
Var X	Percentage of the X variance
W-C	Watson-Crick
WHO	World Health Organisation
XRD	X-Ray crystallography
$ZnCl_2$	Zinc chloride

REKABENTUK, SINTESIS, AKTIVITI SITOTOKSIK DAN INTERKALASI DNA BAGI TERBITAN β-KARBOLINA BARU

ABSTRAK

Fokus kajian ini adalah untuk menyelidik tentang kesan sitotoksik *in vitro* terbitan baru β-karbolina terhadap sel kanser manusia K562. Analisis menggunakan model 3D-QSAR telah mendedahkan kepentingan penukargantian pada posisi-2 dan -9 β-karbolina. Dua siri baru terbitan N^2-benzil-β-karbolina (**M23-M46**) dan N^2-N^9-benzil-1-tertukarganti-β-karbolina (**M47-M113**) telah disintesis dan dicirikan menggunakan tindak balas empat langkah telah memberikan hasil yang baik (>70%). Sebatian **M23-M113** menunjukkan aktiviti antikanser yang paling kuat dengan nilai IC_{50} antara 0.01-4 μM, kecuali sebatian **M88-M90** dengan nilai IC_{50} lebih daripada 100 μM. Enam daripada terbitan N^2-N^9-benzil-1-tertukarganti-β-karbolina (**M53**, **M85**, **M86**, **M104**, **M109** dan **M112**) menunjukkan nilai IC_{50} antara 0.01-0.07 μM berbanding Doxorubicin (DOX) yang digunakan sebagai kawalan positif (0.77 μM). Kajian hubungan struktur-aktiviti (SAR) mendedahkan bahawa penukargantian tambahan kumpulan benzil pada posisi-2 dan -9 menunjukkan aktiviti sitotoksik yang paling menarik. Agen interkalasi seperti DOX, harmine (HAR), 5-fluorouracil (5-FU) dan terbitan β-karbolina yang terpilih, **M53** dan **M56** digunakan sebagai sebatian model. Mekanisme interkalator telah diterokai menggunakan DNA timus anak lembu (CT-DNA) sebagai sistem model. UV-Vis menunjukkan bahawa DOX, HAR, **M53** dan **M56** mendorong kesan hipokromik dan anjakan merah, sementara 5-FU tidak. Dalam pemancaran pendarfluor, pelindapkejutan pendarfluor telah diperhatikan dalam sistem EtBr-DNA (siasatan) dengan penambahan DOX, HAR, 5-FU, **M53** dan **M56**. Dalam dikroisme bulat, DOX dan HAR mengubah keamatan

jalur positif dan negatif DNA dalam arah yang sama manakala sebatian **M53** dan **M56** mencetuskan perubahan yang bertentangan. Pengikatan DOX, HAR, **M53** and **M56** dengan DNA adalah secara mod interkalasi. Dalam kajian in silico, sebatian **M53** dan **M56** telah didok ke d(CGATCG)$_2$ oligonukleotides yang diambil dari Bank Data Protein (PDB ID: 1D12) sebagai wakil model interaksi antara agen antikanser dan DNA melalui mod interkalasi. Kajian eksperimen dan *in-silico* saling dipersetujui di mana kedua-duanya membuktikan bahawa sebatian **M53** dan **M56** terikat kepada DNA secara interkalasi antara pasangan asas CG.

DESIGN, SYNTHESIS, CYTOTOXIC ACTIVITY AND DNA INTERCALATION OF NEW β-CARBOLINE DERIVATIVES

ABSTRACT

The focus of this study has been to investigate the *in vitro* cytotoxic effects of new β-carboline derivatives on the K562 human cancer cell line. Analysis using 3D-QSAR models has revealed the importance of derivatisation at position-2 and -9 of the β-carbolines. Two new series of N^2-benzylated-β-carboline (**M23-M46**) and N^2-N^9-benzylated-1-substituted-β-carboline derivatives (**M47-M113)** were synthesised and characterised using four-step reaction and were produced in good yields (>70%). Compounds **M23-M113** exhibited the most potent anticancer activity with IC_{50} values between 0.01-4 µM, except for compounds **M88-M90** which produced IC_{50} values of more than 100 µM. Six of N^2-N^9-benzylated-1-substituted-β-carboline derivatives (**M53**, **M85**, **M86**, **M104**, **M109** and **M112**) showed IC_{50} values between 0.01-0.07 µM when compared to doxorubicin (DOX) which was employed as the positive control (0.77 µM). The structure-activity relationships (SARs) study has revealed that additional substituents of the benzyl group at position-2 and -9 exhibited the most interesting cytotoxic activities. Intercalator agents such as DOX, harmine (HAR), 5-fluorouracil (5-FU) and selected β-carboline derivatives **M53** and **M56** were used as the model compounds. The intercalating mechanism was explored using calf thymus DNA (CT-DNA) as a model system. UV-Vis showed that DOX, HAR, **M53** and **M56** induced hypochromic effect and redshift, while 5-FU did not. In fluorescence emission, fluorescence quenching was observed in the EtBr-DNA system (probe) upon addition of DOX, HAR, 5-FU, **M53** and **M56**. In circular dichroism (CD), DOX and HAR changed the intensities of the

positive and negative bands of DNA in the same direction while compounds **M53** and **M56** induced the opposite change. The binding of DOX, HAR **M53** and **M56** with DNA was through the intercalation mode. In the *in-silico* study, compounds **M53** and **M56** were docked onto d(CGATCG)$_2$ oligonucleotides retrieved from the Protein Data Bank (PDB ID: 1D12) as the representative of the interaction model through intercalation mode between anticancer agents and DNA. The experimental and *in-silico* studies were in good agreement whereby both proved that compounds **M53** and **M56** were bound to DNA *via* intercalation between CG base pairs.

CHAPTER 1

INTRODUCTION

1.1 Cancer

Cancer, an illness that has haunted mankind and will continue to be a major health issue, can be defined as a collection of diseases characterised by uncontrolled cell proliferation leading to dissemination (metastasis) to other parts of the body eventually compromising normal body function. The spread of the primary growth to secondary locations distinguishes cancer from benign tumours making its eradication far more difficult.

As far as the Malaysian community is concerned, the incidence of cancer increased from 32,000 cases in 2008 to 37,400 in 2012. This number is predicted to rise to 56,932 by 2025 if no action is taken (The Star Online, 2014). According to the International Agency for Research on Cancer (IARC), which is under World Health Organisation (WHO), and through their Globocan project, death due to cancer (cancer mortality) was 20,100 in 2008 and had increased to 21,700 in 2012. Based on statistics released by Globocan 2012, cancer cases worldwide are forecast to rise by 75% and reach close to 25 million over the next two decades (Ferlay et al., 2014; The Star Online, 2014). It is believed that some races are genetically predisposed to particular types of cancer while incidence rates depend on environmental factors such as diet and lifestyle (National Cancer Institute, 2015).

Carcinogenesis, the process leading to cancer formation, is complicated and not yet fully understood and often involves phenotypic alterations that give cancer cells a selective advantage for growth over normal cells. These may include over competitive behaviour for growth factors, over-production of intercellular growth signals or errors in genes which regulate programmed cell death (apoptosis). This is usually accompanied by modifications which enable cells to invade surrounding tissue and metastasize to other parts of the body to form new tumours (King, 1996).

The prognosis for patients treated at the early stages of this malady is invariably better due to the smaller number and less destructive nature of a tumour. Surgery is the usual starting point for treatment of solid tumours followed by radiation therapy and chemotherapy depending on the site and nature of the disease. As a majority of tumour cells have a higher proportion of dividing cells as compared to normal tissue, they are more susceptible to the lethal effect of chemotherapeutic agents. However, rapidly dividing normal cells, such as those of the bone marrow, digestive tract and hair follicles are also affected causing unwanted side effects such as myelosuppression, vomiting, gastrointestinal disturbances and alopecia (Han et al., 2017). This poses limitations on the dose of a particular drug that can be administered, which in turn reduces the effect of the treatment.

The problem of systemic toxicity has been partially alleviated by combination therapy which usually involves the administration of two or three cytotoxic agents with different mechanisms of action, such as topoisomerase inhibitors, antimetabolites, and alkylating agents (Tacar et al., 2012). This strategy also enhances overall tumour cell destruction but rarely eradicates all the cells. The small clone and progenitor cells which survive treatment frequently redivide to form a new,

drug-resistant tumour. Unfortunately, this means that except for prostate cancer, Hodgkin's lymphoma and childhood leukaemia, the disease is often fatal.

As a consequence, extensive research is being carried out to find new drugs that overcome the problems of toxicity and resistance associated with chemotherapy. Many of these are based on compounds already in clinical use.

1.2 DNA intercalating agents

Among the agents currently used in the treatment of cancer are the DNA intercalating agents. These possess a polycyclic aromatic ring system that allows reversible non-covalent interdigitation between adjacent base pairs in the hydrophobic interior of the DNA double helix (Lerman, 1961). The impact would be a local distortion and an overall lengthening of the DNA helix as it unwinds to accommodate the drug molecule (Waring, 1979; Reinert, 1983) (Figure 1.1). Compounds with tri-and tetracyclic chromophores which are approximately of the same dimension as the purine-pyrimidine base pairs usually show optimal binding.

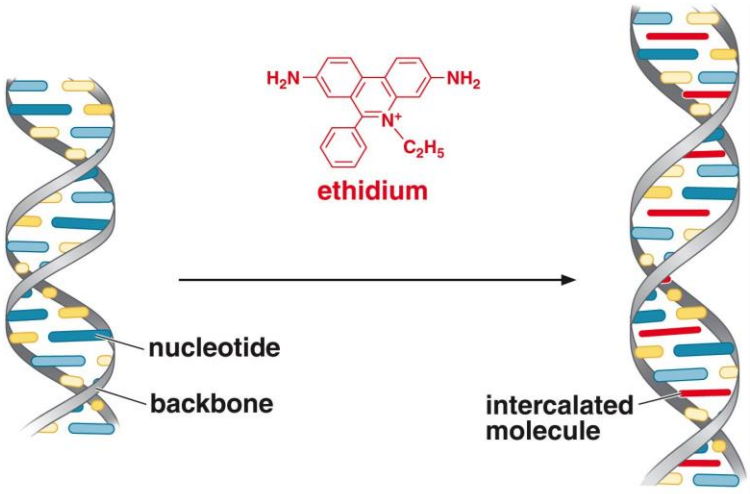

Figure 1.1: Intercalation of ethidium bromide (EtBr) into-double-stranded DNA, showing lengthening of the DNA helix (reproduced from Watson, 1987)

In some cases, the drug may contain additional constituents attached to the chromophore which strengthens intercalation by interacting with the anionically charge DNA phosphate backbone (Foye et al., 1982; Pachter et al., 1982; Pohle et al., 1990). However, this type of binding is much weaker than intercalation because it occurs on the exterior surface of the DNA helix and is influenced to no small extent by the conditions of the surrounding medium (Jones et al., 1980).

1.2.1 The anthracycline antitumor agents

Anthracycline antibiotics such as doxorubicin (DOX) were isolated from Streptomyces bacterium (*Streptomyces peucetius var caesius*) in the 1960s (Chen et al., 1999). DOX still among the most widely and active chemotherapeutic agents in use (Lown, 1993; Iwaki et al., 2000; Minotti et al., 2004; Peng et al., 2005).

Chemically, the anthracyclines contain an amino sugar attached to an aglycone ring, the latter consisting of a non-aromatic (A) ring conjugated with an anthraquinone moiety (Figure 1.2). DOX can also be used alone or in combination to treat a wide range of cancers including acute leukaemias, Hodgkin's and non-Hodgkin's lymphomas, cancers of the bladder, stomach, breast, lung, thyroid, ovaries, soft tissue, bone sarcomas, multiple myelomas, and others (Rebecca et al., 2017).

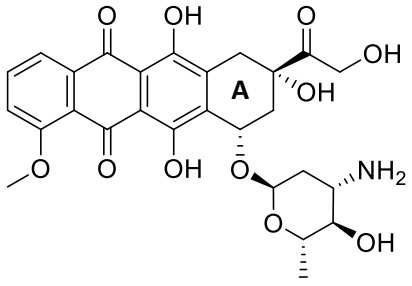

Figure 1.2: The antitumor anthracycline doxorubicin

The principal mode of action of the anthracyclines is thought to be mediated through intercalation of the aglycone portion of the molecule between adjacent DNA base pairs (Takahashi & Naganuma, 2017). DOX interacts with DNA on a molecular level by intercalation and destruction of macromolecular biosynthesis. This inhibits the function of enzyme topoisomerase II which is involved in the unwinding of supercoiling of DNA for transcription. DOX stabilises the topoisomerase II complex after it has fragmented the DNA strand for replication preventing the DNA double helix from being re-sealed thereby stopping the replication process. The aromatic chromophore of the molecule intercalates between the base pairs of the DNA, while the six-membered daunosamine sugar is placed in the minor groove and interacts with flanking base pairs together to the intercalation site (Box, 2007). As a result of the highly undesirable features associated with the use of the anthracyclines in chemotherapy, a lot of time and effort has been devoted to developing derivatives of DOX in the hope of enhancing antitumor activity and lowering the side effects.

In order to elucidate the desired biological activity, the structure of a drug should be complementary with the receptor. However, due to the complex nature of the biological systems, the predicted effect of the structural fluctuations in the biological activity of the drug is uncertain (Shah et al., 2010). Therefore, extensive research is an important pre-requisite for the determination of structure-activity relationship (SAR) and the significance of structural modification. With this in mind, new anticancer agents, β-carbolines, were evaluated for their drug-DNA binding.

In recent years, β-carboline derivatives have been reported to have excellent anticancer drug properties. Their ability to act as DNA intercalating agents is related to their potent antitumor activities (Rescifina et al., 2014; Zhang & Sun, 2015; Kumar et al., 2017). Among the β-carboline derivatives, the most represented

naturally occurring β-carboline alkaloid endowed with antitumor properties is harmine (HAR) or 7-methoxy-1-methyl-9*H*-pyrido[3,4-*b*]indole (Figure 1.3). HAR is capable of inducing DNA single or double strand breaks (Boeira et al., 2002). Recently, derivatives of HAR have come into focus as they can inhibit various cancer cell lines in nanomolar concentrations (Meinguet et al., 2015; Geng et al., 2018).

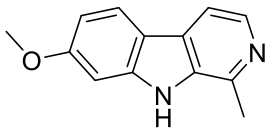

Figure 1.3: The chemical structure of harmine

1.3 Problem statement

Inspired by cytotoxic potential of β-carboline derivatives against various cancer cell lines (Cao et al., 2010; 2013; Zhang et al., 2013), a series of new β-carboline derivatives were designed, synthesised, and screened for their *in vitro* cytotoxic strength.

Previous studies have reported more complicated synthesis route for the β-carboline derivatives with structural requirements for position-2 and -9 (Zhang et al., 2013). Therefore, the present study has been streamlined to develop a more straightforward, less time consuming and cost-effective synthesis route. This synthesis process is challenging especially when it comes to completing aromatization under oxidative conditions and β-carbolineum salt reactions for generating a high yield of β-carboline derivatives. Although the cytotoxic potency at various positions has been explored extensively over the years, synthesis of derivatives with such structural requirements at position-2 and -9 in the one-pot

reaction has not been investigated thus far. Benefits of this reaction include time, cost and labour efficiencies.

For the cytotoxicity studies, literature has reported anticancer potential of β-carboline against many *in vitro* cell lines such as BGC-823, MCF-7, 22RV1, HepG2, 769-P, HT-29, A375, SK-OV-3, Eca-109 and LLC (Zhang et al., 2013). The current study will focus on the structural requirements of β-carboline derivatives at position-2 and -9 for the cytotoxic activity against the K562 cell line. K562 is human immortalised myelogenous leukemia (CML) cell line. There is no cytotoxic activity of β-carboline against K562 has been reported. Therefore, this study is the first of its kind to indicate the structural relationship between β-carboline derivatives and K562 cells. In addition, the orientation of β-carboline derivatives that bind to the DNA complex will also be studied. The interactions between β-carboline derivatives and DNA will be studied using various spectrophotometric methods. In order to understand the molecular interaction with its macromolecular target, molecular docking technique will be used to provide molecular interaction information between β-carbolines and DNA.

1.4 Scope of study

The primary goal of this research is to design and synthesise new β-carboline derivatives library and to elucidate their antitumor structure-activity relationships (SARs). It is essential to use inexpensive starting materials with minimal usage of chromatography and less reaction steps in the synthesis. In the present study, exploration of the cytotoxic potential of β-carboline derivatives having substituents at position-2 and -9 positions was undertaken using 3D-QSAR studies.

The new β-carboline derivatives were produced by the positional modification of benzyl substituent moieties at position-2 and -9. This amendment may be the key for the modulation of cytotoxic strength. The mechanism of action of the compounds *via* DNA binding interactions was analyzed using several analytical procedures including thermal melting denaturation, UV-Visible absorption spectroscopy, fluorescence emission spectroscopy and circular dichroism coupled with the computational technique of molecular docking.

1.5 Objectives

Based on the importance of β-carboline, the objectives of this study are listed below:

i. To understand structural requirement for various positions of β-carboline scaffold as potent cytotoxic agents using 3D-QSAR model developments using literature data.

ii. To synthesise, characterise and evaluate various β-carboline derivatives against human chronic myelogenous leukaemia (CML) cancer cell (K562) and mouse embryonic fibroblast BALB/3T3 clone A31 non-cancer cell line cytotoxic activities.

iii. To investigate the interaction between selected β-carboline derivatives and DNA.

CHAPTER 2

LITERATURE REVIEW

2.1 Background of β-carboline

β-Carboline derivatives display a broad range of significant biological activities (King et al., 2000; Arzel et al., 2001; Chen et al., 2009) and their saturated derivatives are a common nucleus in various natural products (Edwanker, 2009). β-Carboline has a common planar tricyclic pyrido[3,4-*b*]indole ring system that belongs to the group of indole alkaloids consisting of a pyridine ring that is bonded to an indole skeleton (Abramovitch & Spencer, 1964; Allen & Holmstedt, 1980).

Consequently, a substitute β-carboline, 9*H*-pyrido[3,4-*b*]indole - also known as norharman (**1**) has been identified as mentioned by IUPAC. The structure of β-carboline is similar to tryptamine with the ethylamine chain connected to the indole ring, producing a three-ringed structure. The structure and the numbering of the β-carboline skeleton are shown in Figure 2.1.

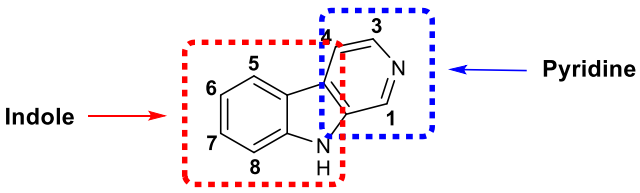

Figure 2.1: Numbering of the β-carboline (**1**) skeleton

The first β-carboline alkaloid known as harmaline (**5**), was initially isolated in 1841 from *Peganum harmala* (Zygophyllaceae, Syrian rue) (Figure 2.2). In North Africa and the Middle East, it is used as an emmenagogue and an abortifacient as well as a traditional herb to stimulate menstrual flow (Mahmoudian et al., 2002). In

the Amazon basin, plants containing β-carbolines were utilised as hallucinogenic snuffs or drinks. Besides, the extracts of the seeds of *Peganum harmala* have been used for hundreds of years to treat malaria and alimentary tract cancers in Northwest China (Chen et al., 2004; Moloudizargari et al., 2013). The roots and seeds of *Peganum harmala* contain the highest level of alkaloids with low concentrations being observed in the leaves and stems. In addition, there is no β-carboline alkaloid in the flowers (Lamchouri, 2014).

Figure 2.2: *Peganum harmala* (adapted from Asgarpanah & Ramenzanloo, 2012)

The occurrence of β-carbolines in nature is widespread presumably due to the simple biogenesis of tryptamine (or tryptophan). During the last two decades, numerous β-carboline alkaloids with saturated and unsaturated tricyclic ring systems have been revealed from various plants, marine creatures, insects, foodstuff and mammals. This also includes body fluids and human tissues as major bioactive constituents (Airaksinen & Kari, 1981; Karin et al., 1990; Saxton, 1998; Carbrera & Seldes, 1999; Kawasaki & Higuchi, 2005; Cao et al., 2007; Higuchi & Kawasaki, 2007; Mansoor et al., 2009; Gonzalez-Gomez et al., 2009).

β-Carbolines can be categorised according to the degree of saturation of their *N*-containing six-membered pyridine ring. Unsaturated members are fully aromatic

β-carbolines such as norharman (**1**), harman (**2**), harmine (**3**) and harmol (**4**), whereas dihydro-β-carbolines (DHβCs) such as harmaline (**5**), harmalol (**6**) and harmalan (**7**) have partially saturated ring (Figure 2.3). Fully saturated members are known as tetrahydro-β-carboline (THβC) such as compound **8** (Figure 2.3) (Cao, et al., 2007). The tricyclic β-carbolines usually contain several substituents both in the *N*-containing six-membered pyrido ring and the indole ring. The so-called Pictet-Spengler condensation reaction of indoleethylamines or tryptophan with an aldehyde or α-keto acids has been confirmed to be the most efficient route for the chemical synthesis of THβCs or tetrahydro-β-carboline-3-carboxylic acids (THβCAs) (Cao et al., 2007). They showed unique three-dimensional arrangements of the chiral functional groups exhibiting specificity in the protein binding and eliciting a specific biological response. The rings are often referred to as A-, B-, and C-ring, as labelled in structure **1** (Figure 2.3).

The presence of two kinds of nitrogen (-N and -NH) in β-carbolines, pyridinic nitrogen and the less crucial pyrrolic nitrogen, affects the photophysical and photochemical properties of the alkaloids. The basicity of pyrrolic nitrogen increases upon excitation (Dias et al., 1992; Carmona et al., 2000) and is also affected by the substitutions in the tricyclic structure (Hidalgo et al., 1990). Depending on the pH and solvent employed, β-carbolines can exist in four forms; cationic, neutral, anionic and zwitterion (or alternative quinine-type canonical formula) (Varela et al., 2001).

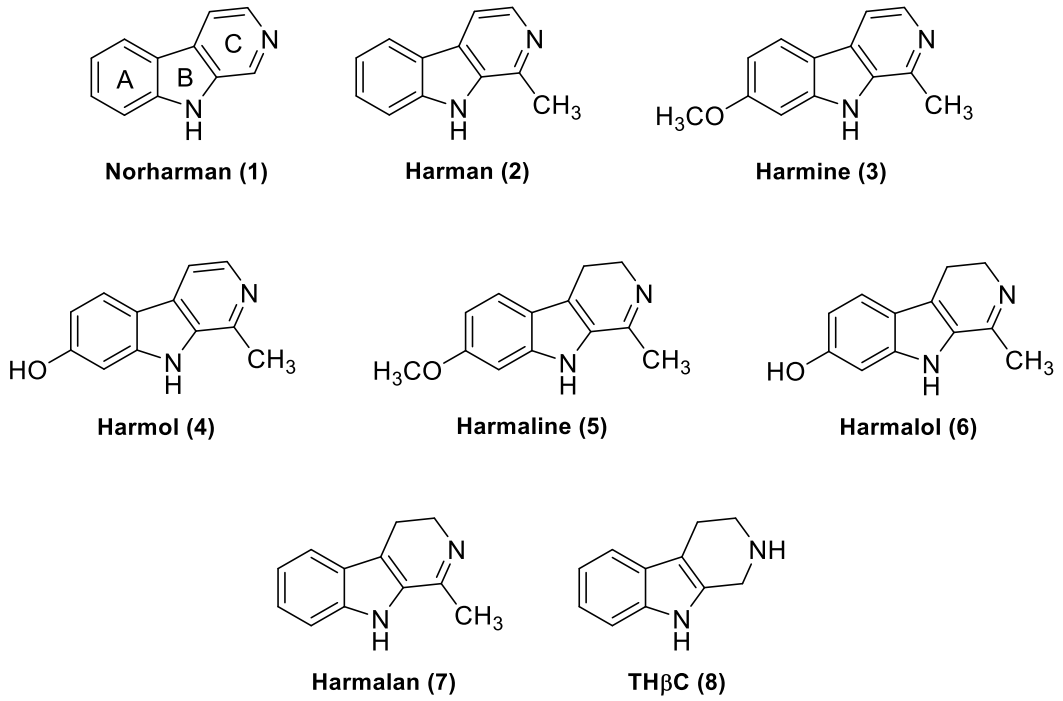

Figure 2.3: Structures of β-carbolines (**1**, **2**, **3** and **4**), dihydro-β-carbolines (DHβCs) (**5**, **6** and **7**) and tetrahydro-β-carboline (THβC) (**8**) alkaloids

β-Carbolines are of great interest due to their broad spectrum of biochemical effects and pharmacological properties. Numerous reports showed β-carboline alkaloids effect the central nervous system (CNS) such as benzodiazepine receptors, 5-HT_{2A} and 5-HT_{2C} receptors (Brierly & Davidson, 2012; Herrick-Davis et al., 2015; Phipps & Grundmann, 2017). Other researches focused on the antitumor activity of β-carbolines. Various reports suggested β-carbolines demonstrate potent antitumor activities (Cao et al., 2013; Zhang et al., 2013). The cytotoxic activity correlates with both the planarity of the molecule and the presence of the ring substituents (Chourasiya et al., 2016). Multiple mechanisms have been suggested for their antitumor activity such as intercalating into DNA (Hayashi et al., 1977), inhibiting topoisomerase I and II (Deveau et al., 2001), cyclin-dependent kinase (CDK) (Song et al., 2002; 2004), and IKK (I-Kappa-B kinase) (Castro et al., 2003).

2.2 Synthesis of β-carboline derivatives

Several synthesis methods aimed at displaying the biological activities of β-carboline derivatives have been reported (Snyder et al., 1948; Brossi et al., 1973; Bobbitt & Willis, 1980; Lippke et al., 1983; Ishida et al., 1999; Cao et al., 2004; 2005a; 2008; 2010a; Guan et al., 2006; Wu et al., 2009a; 2009b; Meesala et al., 2014; Kamal et al., 2015a; 2015b). Their importance has demanded efficient synthesis methods for constructing heterocyclic systems and their functionalization. The most efficient and rapid routes for the construction of the β-carboline moiety include the intramolecular Friedel-Crafts reactions such as Pictet-Spengler and Bischeler-Napieralski reaction followed by esterification, aromatization or decarboxylation and *N*-alkylation or *N*-benzylation.

2.2.1 Precursors in the synthesis of β-carbolines

Tryptophan (**9**) and its decarboxylation product tryptamine (**10**) (Figure 2.4) are two primary precursors usually used in the construction of β-carboline skeleton (Love, 2006; Domínguez & Pérez-Castells, 2011). A recent study has described that indole (**11**) (Figure 2.4) is the source of the β-carboline skeleton (Kamlah et al., 2016).

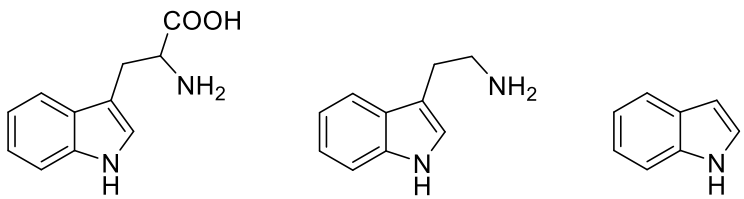

Figure 2.4: Precursors used in the synthesis of β-carbolines

2.2.2 Conventional synthetic methods of β-carbolines

Pictet-Spengler and Bischeler-Napieralski condensations are the two conventional methods used to synthesise β-carbolines (Love, 2006; Cao et al., 2007; Domínguez & Pérez-Castells, 2011). However, these two well-known procedures do not lead directly to the entirely aromatic β-carbolines (**1**) but through tetrahydro- (**8**) or dihydro-β-carboline derivatives (**12**), as illustrated in Scheme 2.1.

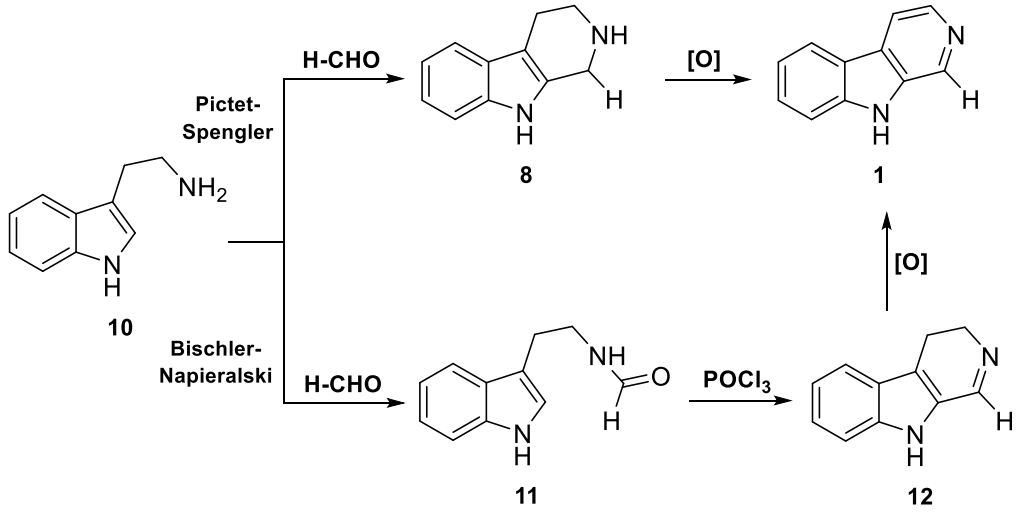

Scheme 2.1: Summary of conventional synthetic methods of β-carbolines (**1**)

The Pictet-Spengler reaction which was first discovered in 1911 by Ame Pictet and Theodor Spengler has been the crucial procedure in generating either substituted or fused β-carbolines (Pictet & Spengler, 1911; Cox & Cook, 1995). It consists of the condensation of indole ethylamine such as tryptamine (**10**) (or tryptophan, **9**) with an aldehyde or another electrophile. The reaction of THβCs proceeds through a spiro-indolenine intermediate (**10b**) as illustrated in Scheme 2.2, which collapses to form β-carbolines (**1**) (Cao et al., 2004).

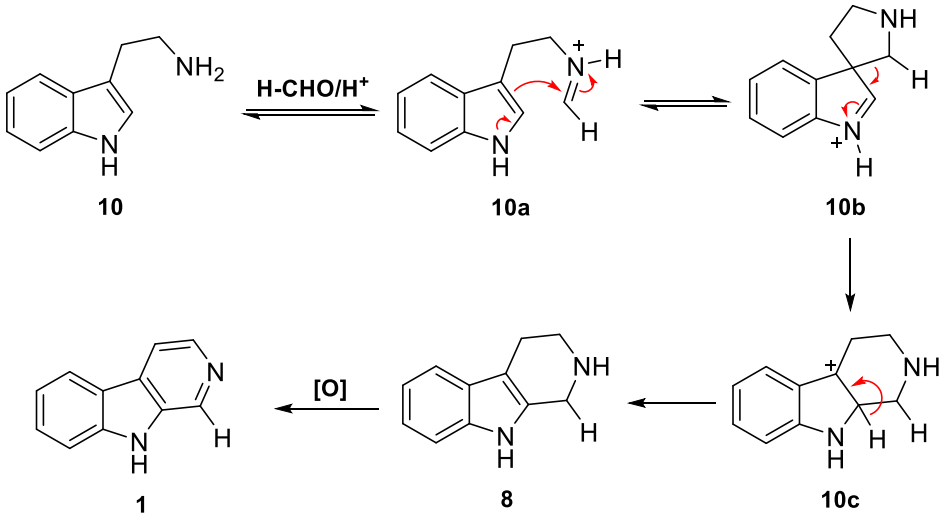

Scheme 2.2: Mechanism reaction of compound **8** using Pictet-Spengler reaction

Nucleophilic aromatic rings such as indole or pyrrole have given products with excellent yields under mild conditions while the less nucleophilic aromatic rings such as benzene or indoles with electron withdrawing substituents on the benzene ring have exhibited poor yields even under harsh conditions. The electrophilic substitution at position-2 by indole gave the five-membered ring intermediate (**10b**) which then rearranged to form a six-membered ring (**10c**). Deprotonation gave the desired product of THβC (**8**) (Larghi et al., 2005). The electrophilicity of the imine double bond works as the driving force for the cyclisation (Scheme 2.2). The reaction occurs readily in mild condition which is temperature- and pH-dependent. Aromatization to the desired β-carbolines (**1**) can be accomplished by the oxidation of THβC (**8**).

Bischeler-Napieralski reaction is an intramolecular electrophilic aromatic substitution reaction that allows the cyclisation of β-arylethylamides. It was first discovered in 1893, by August Bischler and Bernard Napieralski. This result is similar to the Pictet-Spengler reaction but differs in the fact that tryptamine (**10**) is first acylated to give amide (**11**) (Scheme 2.3). The latter is dehydrated to an active

iminium species which is then cyclised to provide DHβC (**12**). The common dehydration reagents used were PCl_5, $POCl_3$, $SOCl_2$ or $ZnCl_2$ for the removal of the carbonyl oxygen. Even though the oxidation step of the DHβC (**12**) is much easier to achieve than THβC (**8**) the dehydration step requires vigorous reaction conditions which restrict the use of this method.

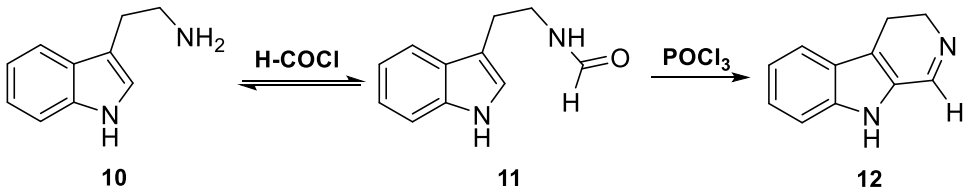

Scheme 2.3: A Bischler-Napieralski cyclisation and reduction of DHβC (**12**)

2.2.3 The aromatization of β-carbolines system

The Pictet-Spengler reaction allows for the construction of a THBC core with appropriate substitution which could be extended after the cyclisation or the installation of different changes, undergoing cascade reactions during cyclisation to afford new THBC derivatives. These THBCs can then be oxidised to generate the desired β-carboline derivatives.

However, alternative strategies to create β-carbolines can also be accomplished by using a variety of reagents (Love, 1996). A few reactions have been conducted by heating the substrate with palladium on carbon (Soerens et al., 1979; Coutts et al., 1984; Hibino et al., 1985), sulphur in refluxing cumene or xylenes (Cain et al., 1982; Cao et al., 2004; Wu et al., 2009a; Qifeng et al., 2009), and potassium dichromate over the extended reaction time (Zhang et al., 2013). Other oxidising agents such as selenium dioxide (Gatta & Mitisi, 1987; Cain et al., 1983) and manganese dioxide (Dantale & Soderberg, 2003) were often used in excess. These organic-based reagents affect such dehydrogenation limiting the choice to only

the quinone-derived reagents such as chloranil (Snyder et al., 1948; Lippke et al., 1983), 2,3-dichloro-5,6-dicyano-1,4-benzoquinone and DDQ (Kobayashi et al., 1990; Yeun-Mun & Hamann, 2007) with low yields (< 30%).

A more efficient method for the synthesis of β-carbolines employing one-pot tandem β-elimination and aromatization reactions has been developed (Dong et al., 2010). The plausible mechanism for the one-pot conversion is shown in Scheme 2.4 converting *N*-tosyl-THBCs (**13**) into β-carbolines (**14**) with 70-95% yields (Dong et al., 2010). The *N*-tosyl-THBCs (**13**) would first react with a base to form the anions **A-1** or **A-2**, and these would then immediately undergo β-elimination to afford the dihydro intermediates **B-1** or **B-2** (Amos et al., 2003; Ishikawa et al., 2004; Kitahara et al., 2008). The dihydro intermediates, **B-1** or **B-2,** would then be oxidized *in situ* by molecular oxygen in the air to give the final product of β-carbolines (**14**) (Previero et al., 1984). The reaction pathways would be governed by the acidities of the protons on C-1 and C-3, whereby if the proton on C-1 was more acidic, then **Path A** would be preferred, whereas if the proton on C-3 were more acidic, **Path B** would be preferred.

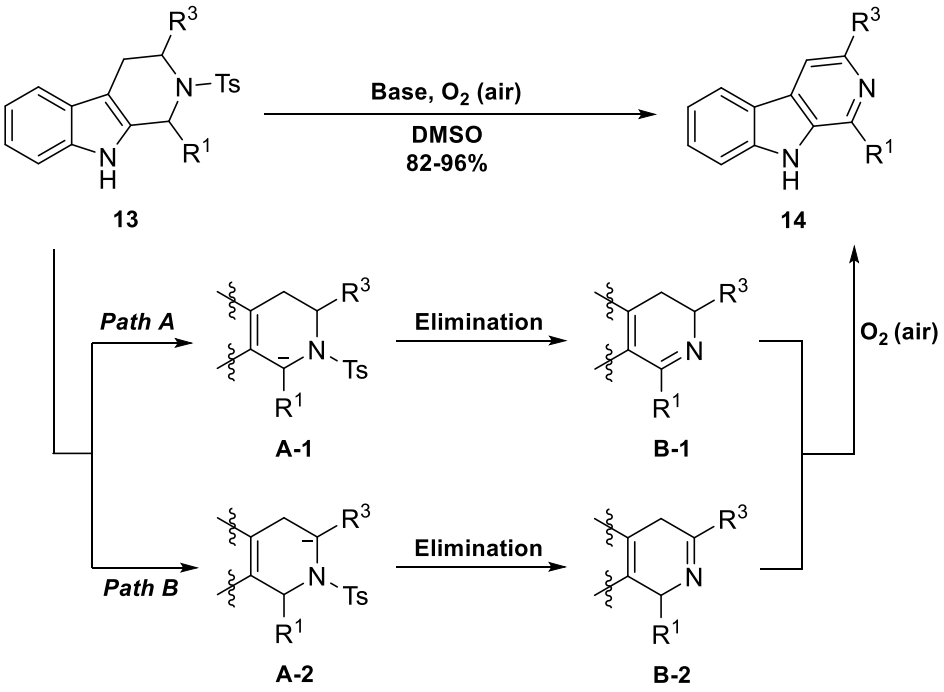

Scheme 2.4: A plausible mechanism for the one-pot conversions of *N*-tosyl-THBCs (**13**) into β-carbolines (**14**) through tandem β-elimination and aromatization reactions

Another work reported the aromatization of THβCs under different conditions. Panarese & Water (2010) showed that 2-iodoxybenzoic acid (IBX) is a convenient reagent for the dehydrogenation of THβCs (**15**). They applied this approach in the total synthesis of marine indole alkaloid Eudistomin U (**17**) as shown in Scheme 2.5 (Panarese & Water, 2010).

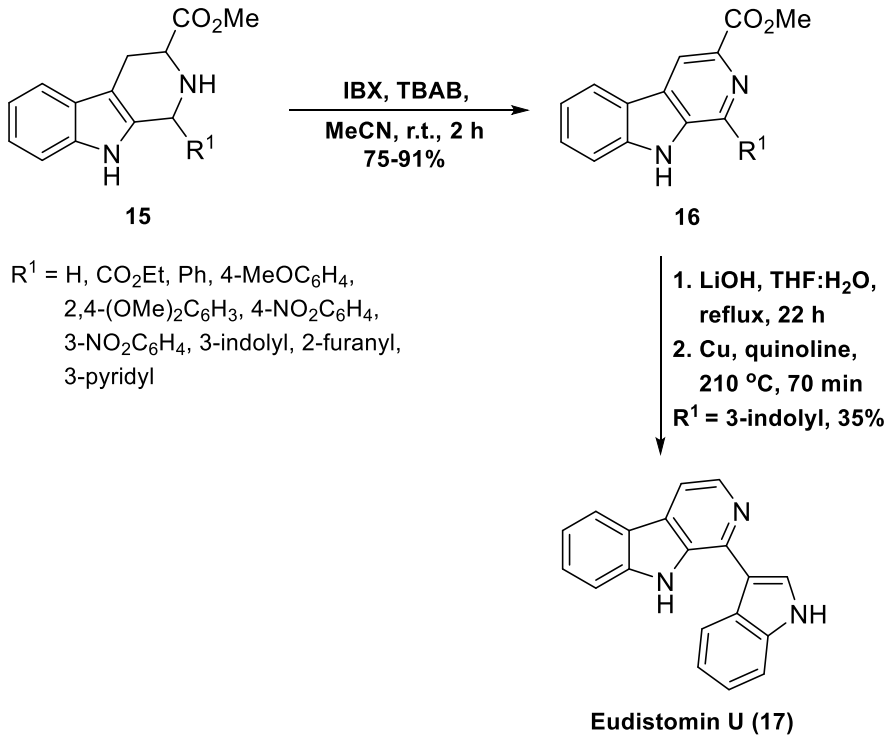

Scheme 2.5: IBX-mediated aromatization in the total synthesis of Eudistomin U (**17**)

Meesala et al. (2014) reported an efficient synthetic method to construct aromatic β-carbolines (**1**) from THβCAs (**18**) *via* copper(II) mediated decarboxylation and subsequent aromatization. Based on previous reports (Cohen & Schambach 1970; Goossen et al., 2007), a possible mechanism has been outlined in Scheme 2.6. Initially, a copper catalyst is inserted into a carboxylic acid (**18**) to give an intermediate **18a** which undergoes oxidative addition to form intermediate **18b**. A rapid reductive elimination provides the intermediate decarboxylation **18c**, followed by protonolysis and converting it into THβCs (**8**), which is then transformed into the aromatic β-carboline (**1**) by oxidative aromatization.

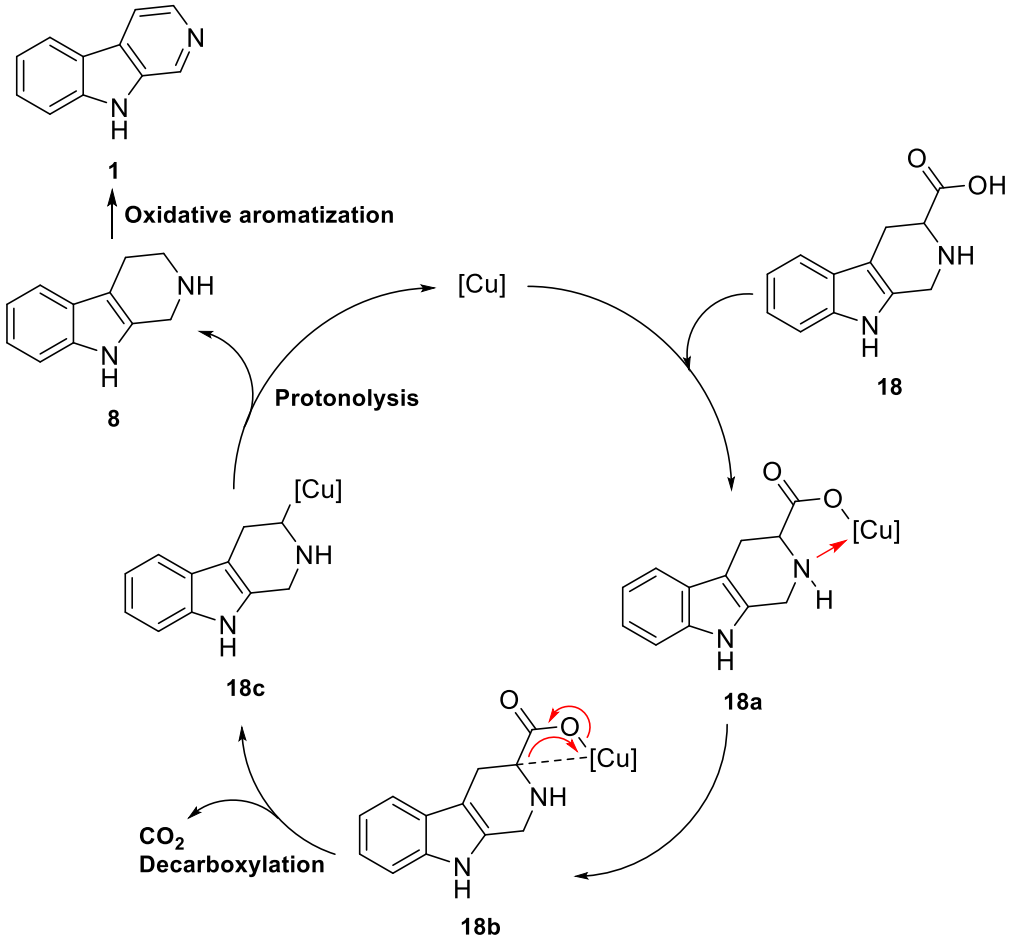

Scheme 2.6: Proposed mechanism for copper-mediated decarboxylation and aromatization of THβCAs (**18**)

Kamal et al. (2015a, b) developed a simple, mild and efficient protocol for a one-pot reaction of a THβACs (**19**) to produce β-carboline (**20**) (Scheme 2.7). This employs a cost-effective or mild oxidant *N*-chloro-succinimide (NCS) (Kamal et al., 2015a) and iodobenzene diacetate (Kamal et al., 2015b) (Scheme 2.8), which produces high yields of the desired products and is able to serve as an alternative method compared.

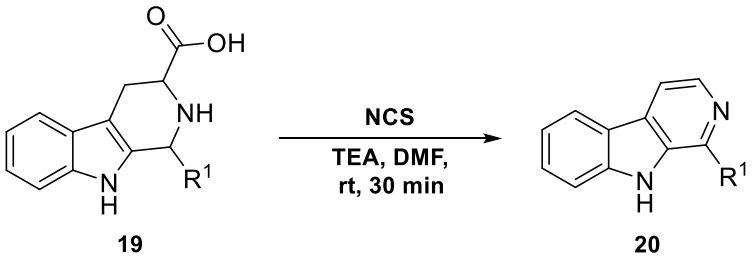

19 20

Mechanism:

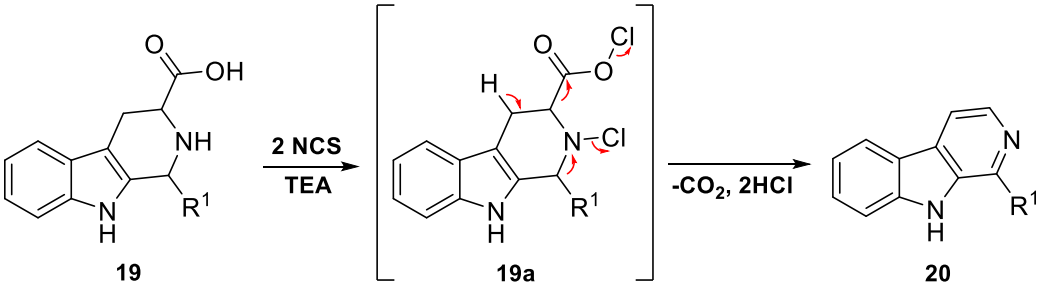

19 19a 20

Scheme 2.7: A possible reaction mechanism for the decarboxylation aromatization of THβCs (**19**)

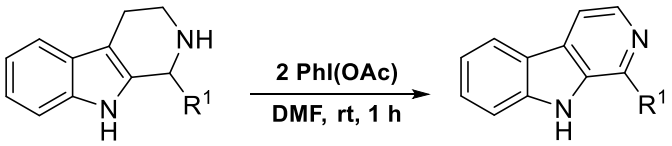

21 20

Scheme 2.8: Synthesis of β-carbolines (**20**) from THβCs (**21**) using iodobenzene diacetate

To summarize the aromatization of β-carboline derivatives, a variety of methods have been used, but only limited forms can generate the essential 1-substituted product. An oxidation step is also necessary to prepare the entirely aromatic β-carbolines from DHβCs (**12**). Since the oxidation of DHβC (**12**) is more facile than THβCs (**8**), there is a drawback in the Bischeler-Napieralski approach (Scheme 2.1, page 14) which needs a vigorous condition in the dehydration reaction leading to **8** thereby making the Pictet-Spengler reaction the most appropriate strategy for this project.

2.3 Pharmacological effects of β-carboline derivatives *in vitro*

Detailed knowledge relating to the pharmacophore of a given substance enhances the understanding of the mechanism. It is possible to identify the features of the pharmacophore that increase the activity of the ligand in comparison to its derivatives. Several investigations have reported the effects of β-carboline alkaloids on the CNS. In the last decade, interest in these alkaloids was stimulated by their promising antitumor activities. 7-Methoxy-β-carboline scaffold, harmine (**3**) binds to DNA one hundred-fold more efficiently than harmaline (**5**) showing cytotoxicity and antitumor activities against HL-60 and K562 cells (Ishida et al., 1999; Patel et al., 2012).

Ishida et al. (1999) reported that twenty-six β-carbolines were evaluated for *in vitro* cytotoxicity in a human tumour cell line panel with structural modifications at position-1, -2, -3, -6, -7 and -9. Harmine (**3**) exhibited significant activities against several cell lines including three drug-resistant KB sublines with various resistance mechanisms. α-(4-Nitrobenzylidine)-harmine (**22**) showed a broad cytotoxicity spectrum against ovarian cancer (1A9), nasopharynx (KB), osteosarcoma (SaOS-2), lung carcinoma (A549), melanoma cancer (SK-MEL-2), glioblastoma (U-87-MG) and breast cancer (MCF-7) cells with ED_{50} values ranging from 0.3 to 1.2 µg/mL. SAR analysis suggested that; (i) the introduction of an oxygenated substituent at C-7 led to the enhanced cytotoxic activity; (ii) the length of C-7 alkoxy chain affected both the cytotoxicity and cell line specificity; (iii) N^9-alkylated-β-carboline derivatives exhibited strong cytotoxic effect; (iv) C-6 brominated-β-carboline derivatives showed selective cytotoxic activities; (v) N^2-alkylated-β-carboline derivatives displayed distinct cytotoxic activities; (vi) 3,4-dihydro-β-carboline derivatives were inactive (Ishida et al., 1999).

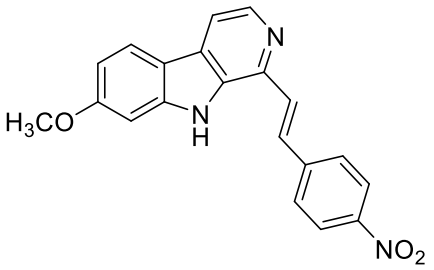

22

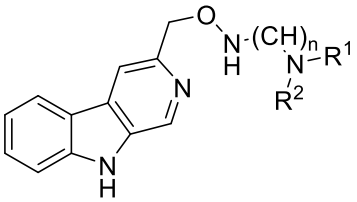

23: n = 2, R^1 = H, R^2 = H
24: n = 2, R^1 = C_2H_5, R^2 = C_2H_5
25: n = 4, R^1 = H, R^2 = H
26: n = 4, R^1 = CH_3, R^2 = CH_3
27: n = 6, R^1 = H, R^2 = H

Xiao et al. (2001) have reported that 3-substituted-β-carboline derivatives, **23-27** showed cytotoxic activities against human tumour cell lines including HL-60, KB, Hela and BGC-823 and were also bound to DNA by intercalation. Compound **25** exhibited the strongest stabilisation of CT-DNA (ΔT_m = 5.7 °C), the most significant binding affinity (K_b = 4.503 × 10^4 M^{-1}) as well as the lowest binding energy and showed high inhibition rate for HL-60 and BGC-823 cells.

Bis-3,4-dihydro-β-carbolines (**28**) and bis-β-carbolines (**29**) were synthesised and exhibited cytotoxic activity towards L-1210 cell with IC_{50} values less than 4 μM (Jiang et al., 2002). Also, 1-substituted-3,4-dihydro-β-carboline derivatives showed significant antitumor activities against human KB-16 and murine P-388, HT-29 and A-549 (Al-Allaf & Rashan, 1998). Among them, 1-(9'-ethyl-3'-carbazole)-3,4-dihydro-β-carboline (**30**) exhibited the most potent cytotoxic activities against all tested tumour cell lines with IC_{50} < 0.001 ug/ml (Shen et al., 2005). It is worthy to note that *trans*-palladium(II)-harmine complexes (**31**) displayed remarkable cytotoxic activities against P-388, L-1210 and K562 cell lines with the IC_{50} of 0.385, 0.385 and 0.364 μM, respectively (Al-Allaf & Rashan, 1998).

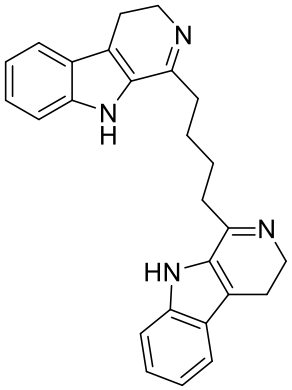

28

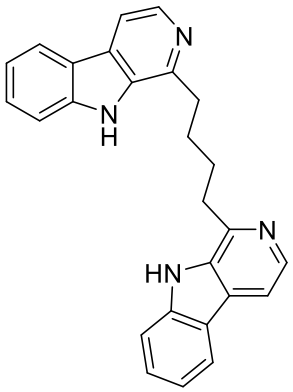

29

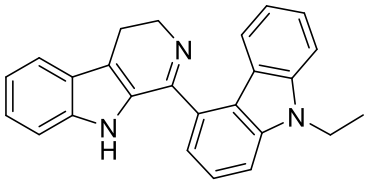

30

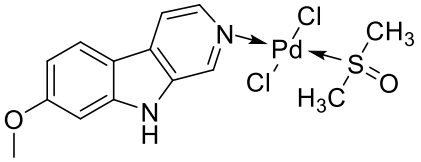

31

Cao and co-workers previously synthesised various β-carboline derivatives by simple structural modifications and probed the fundamental requirement of these compounds for potent activity *in vitro* (Cao et al., 2004; 2005; 2005a; 2008). A series of new 9-substituted-β-carboline derivatives were synthesised from harmine (**1)** and L-tryptophan (**9**). Compound **32** with carboxyl and *n*-butyl groups at position-9 and -3, respectively, showed the highest antitumor effect against human tumour cell lines including PLA-801 with IC_{50} value of 92 µM, HepG2 (73 µM) and Bel-7402 (92 µM), BGC-823 (116 µM), Hela (60 µM) and Lovo (11 µM) (Cao et al., 2004). Later, other series of new 1,3-bisubstituted- and 1,3,9-trisubstituted-β-carbolines were synthesised and evaluated for *in vitro* study against human tumour cell lines including PLA-801, HepG2, Bel-7402, BGC-823, Hela and Lovo (Cao et al., 2005a). 1,3,9-Trisubstituted β-carboline derivatives showed higher cytotoxic activities *in vitro* than their corresponding 1,3-bisubstituted derivatives. Among all the synthesised compounds, 1,3,9-trisubstituted-β-carbolines (**33)** with a methyl group at position-1, ethoxycarbonyl group at position-3 and pentafluorobenzyl at position-9